P2Y2R contributes to the development of diabetic nephropathy by inhibiting autophagy response

Theodomir Dusabimana [1,2], So Ra Kim [1], Eun Jung Park [1], Jihyun Je [1], Kyuho Jeong [1], Seung Pil Yun [1,2], Hye Jung Kim [1,2], Hwajin Kim [1,*], Sang Won Park [1,2,**]

ABSTRACT

Objective: Diabetic nephropathy (DN) is one of the most common complications of diabetes and a critical risk factor for developing end-stage renal disease. Activation of purinergic receptors, including P2Y2R has been associated with the pathogenesis of renal diseases, such as polycystic kidney and glomerulonephritis. However, the role of P2Y2R and its precise mechanisms in DN remain unknown. We hypothesised that P2Y2R deficiency may play a protective role in DN by modulating the autophagy signalling pathway.
Methods: We used a mouse model of DN by combining a treatment of high-fat diet and streptozotocin after unilateral nephrectomy in wild-type or P2Y2R knockout mice. We measured renal functional parameter in plasma, examined renal histology, and analysed expression of autophagy regulatory proteins.
Results: Hyperglycaemia and ATP release were induced in wild type-DN mice and positively correlated with renal dysfunction. Conversely, P2Y2R knockout markedly attenuates albuminuria, podocyte loss, development of glomerulopathy, renal tubular injury, apoptosis and interstitial fibrosis induced by DN. These protective effects were associated with inhibition of AKT-mediated FOXO3a (forkhead box O3a) phosphorylation and induction of FOXO3a-induced autophagy gene transcription. Furthermore, inhibitory phosphorylation of ULK-1 was decreased, and the downstream Beclin-1 autophagy signalling was activated in P2Y2R deficiency. Increased SIRT-1 (sirtuin-1) and FOXO3a expression in P2Y2R deficiency also enhanced autophagy response, thereby ameliorating renal dysfunction in DN.
Conclusions: P2Y2R contributes to the pathogenesis of DN by impairing autophagy and serves as a therapeutic target for treating DN.

1. INTRODUCTION

Diabetic nephropathy (DN) is a chronic complication of diabetes and is associated with an increased morbidity and mortality in patients with both type 1 and type 2 diabetes worldwide [1]. Clinically, DN is characterised by overt proteinuria, elevated plasma creatinine and a decline in the glomerular filtration rate (GFR). Early stages of DN exhibit podocyte loss, glomerular hypertrophy, mesangial matrix expansion and glomerular basement membrane thickening, while advanced stages of DN exhibit nodular glomerulosclerosis, mesangiolysis and tubulointerstitial fibrosis [2,3]. Although the current management of tight glycaemic control and renin-angiotensin system blockade slow the progression of DN, many diabetic patients still progress to chronic kidney diseases (CKD) and eventually end-stage renal disease (ESRD) [4]. Thus, elucidating the mechanisms that mediate the early stages of DN may help to identify a novel therapeutic target for preventing the development and progression of DN.

Autophagy is a highly conservative cellular process that degrades and recycles misfolded or dysfunctional proteins and damaged organelles to maintain cellular homeostasis via the lysosome pathway [1,5]. Autophagy is regulated through the nutrient-sensing signalling pathways, which are altered in diabetes due to metabolic stress [6]. Previously, autophagy deficiency was reported to contribute in the progression of DN [7,8]. As a transcription factor, FOXO3a (forkhead box O3a) regulates cellular processes, including autophagy, metabolism, cell proliferation, apoptosis and aging [9]. The FOXO3a activity is precisely regulated by post-translational modification, such as phosphorylation and acetylation [10]. Sirtuin-1 (SIRT-1) deacetylates FOXO3a, which enhances FOXO3a-induced transcription of autophagy and antioxidant genes, while suppressing FOXO3a-induced apoptosis [9,11]. Diabetes-induced downregulation of SIRT-1 leads to inhibition

[1]Department of Pharmacology, Institute of Health Sciences, Gyeongsang National University School of Medicine, Jinju 52727, Republic of Korea [2]Department of Convergence Medical Sciences, Institute of Health Sciences, Gyeongsang National University Graduate School, Jinju 52727, Republic of Korea

*Corresponding author. Department of Pharmacology, Institute of Health Sciences, Gyeongsang National University College of Medicine, 15, 816 Beon-gil, Jinjudaero, Jinju 52727, Republic of Korea. Fax: +82 55 772 8079. E-mail: hwajin1@gmail.com (H. Kim).

**Corresponding author. Department of Pharmacology and Convergence Medical Sciences, Institute of Health Sciences, Gyeongsang National University College of Medicine, 15, 816 Beon-gil, Jinjudaero, Jinju 52727, Republic of Korea. Fax: +82 55 772 8079. E-mail: parksw@gnu.ac.kr (S.W. Park).

of FOXO3a signalling, resulting in reduced autophagy and accelerating the pathogenesis of DN [1,8]. Therefore, the crosstalk of SIRT-1 and autophagy might be a therapeutic target for preventing and treating DN. However, the precise molecular mechanisms are not fully understood.

Nucleotides are the key subunits for nucleic acids to provide the energy for intracellular metabolism. They can be released, in the form of ATP or UTP, from the cells to act physiologically as extracellular second messengers or pathologically as danger signals [12]. The extracellular ATP, ADP, UTP or UDP was found to activate purinergic P2 (P2Y) receptors, which are subdivided into eight P2Y receptors (P2Y1, P2Y2, P2Y4, P2Y6 and P2Y11-14). Particularly, P2Y2R is expressed in the glomerular, mesangial, podocyte and renal tubule cells [12,13]. Activation of P2Y2R on these cells is associated with a broad range of cellular responses, including release of cytokines, production of ROS, apoptosis, chloride secretion, cell proliferation and vascular remodelling [13—17].

Previously, it has been reported that the expression of P2Y2R is upregulated during polycystic kidney disease and promotes cyst formation and growth. Accordingly, P2Y2R knockdown reduces cyst expansion and improves renal function [18,19]. Genetic deletion of the P2Y2R ameliorates the development of lithium-induced polyuria [16]. Moreover, increased ATP release induced by hyperglycaemia contributes to mesangial extracellular matrix expansion in diabetes [20]. Other P2Y receptors have been investigated in the pathogenesis of renal diseases. For instance, P2Y1R deficiency protected against renal capillary loss, fibrosis and apoptosis in a crescentic glomerulonephritis model [21]. Moreover, P2Y6R activation enhanced inflammatory response in a peritonitis model, which was abolished in P2Y6 null mice [22]. These findings related to purinergic receptor signalling proved that targeting P2Y2R might be a potential avenue to treat renal diseases.

Recently, it was reported that P2Y2R activation contributes to the progression and onset of glomerulonephritis and CKD [23,24]. However, the role of P2Y2R in the pathogenesis of DN remains unknown. In this study, we investigated whether P2Y2R deficiency may play a protective role, particularly by modulating the autophagy signalling pathway in DN. For the first time, we demonstrated that P2Y2R deficiency restores the autophagy response and protects against glomerular and tubular injury and interstitial fibrosis induced by DN through the regulation of AKT/FOXO3a and SIRT-1 signalling.

2. MATERIALS AND METHODS

2.1. Experimental animals

Wild-type (WT) C57BL/6 mice (7 weeks old) were purchased from Koatech Co. (Pyeongtaek, South Korea), and homozygous P2Y2R knockout (KO) male mice on C57BL/6 background (strain B6.129P2—P2ry2tm1Bhk/J) were obtained from Jackson Laboratory. All mice were maintained in the animal facility at Gyeongsang National University. All animal experiments were approved by the Institutional Board of Animal Research at Gyeongsang National University and performed according to the National Institutes of Health guidelines for laboratory animal care. Mice were housed with an alternating 12-h light/dark cycle and provided with water and standard chow ad libitum.

2.2. DN animal model

We used a DN model by combining unilateral nephrectomy (UNx), high-fat diet (HFD) and streptozotocin (STZ) treatment in C57BL/6 male mice to accelerate DN, as we previously described [25]. WT and P2Y2R KO mice were habituated for 1 week and subjected to UNx. After 2 days,

the mice were fed with a normal chow diet (WT or KO control, n = 8) or a HFD (60 Kcal % fat; Research Diets, Inc., New Brunswick, NJ, USA). After 3 weeks, STZ (100 mg/kg) was intraperitoneally injected to HFD-fed mice (WT or KO DN, n = 14). Hyperglycaemia was confirmed by measuring fasting blood glucose level from the tail vein using an Accu-Chek glucometer (Roche Diagnostics, Mannheim, Germany). At 6 weeks post-STZ injection, all mice were sacrificed, and the right kidney was removed and weighed. Each kidney half was snap-frozen in liquid nitrogen for storage at −80 °C or fixed in 10% buffered formalin for further analysis. Blood was collected from an inferior vena cava using a heparinized syringe, centrifuged at $3000 \times g$ for 20 min and the supernatants stored at −80 °C for biochemical analysis.

2.3. Biochemical assays

Plasma creatinine was measured by a direct colorimetric Jaffe method and detected using a spectrophotometer (Shimadzu UV-1800 spectrophotometer, Tokyo, Japan), as previously described [25]. Blood urea nitrogen (BUN) was measured using a commercial assay kit from IVDLab (Uiwang, Republic of Korea). Urine samples were collected from each mouse housed in a metabolic cage (Jeungdo Bio & Plant Co., Seoul, Republic of Korea) for 16 h before sacrifice. Urine volume from each mouse was measured and centrifuged at $2000 \times g$ for 10 min to precipitate the sediments. Then the supernatant was transferred into a sterile tube for storage at −80 °C. Urine albumin and creatinine were determined by commercial assay kits from Abcam (Cambridge, MA, USA) according to the manufacturer's instructions. Urine albumin excretion was presented by urine albumin-to-creatinine ratio (UACR), a ratio calculated by urine albumin being divided by absolute urine creatinine levels.

2.4. Measurement of ATP levels

ATP release to the extracellular space was measured in the fresh plasma collected from each mouse by the ENLITEN® ATP assay system bioluminescence detection kit (Promega, Madison, WI, USA) according to the manufacturer's instructions. The ATP levels were determined by the Glomax® 20/20 luminometer (Promega) and calculated based on an ATP standard curve.

2.5. Periodic Acid—Schiff (PAS) and Picro-Sirius Red staining

Formalin-fixed kidney tissues were embedded in paraffin and sectioned at 5 μm of thickness. Kidney sections were stained with PAS staining (Abcam) for histological analysis and Picro-Sirius Red staining (Abcam) for visualisation of collagen deposition. All stainings were performed by following the standard protocols. All images were captured using a CKX41 light microscope (Olympus, Tokyo, Japan).

2.6. Kidney histological examination

Renal histological abnormalities were assessed semi-quantitatively as previously described [26—28]. After PAS staining, the severity of glomerular injury was evaluated in randomly selected fields at $400 \times$ magnification and graded as follows: grade 0 = normal, grade 1 = <25%, grade 2 = 25—50%, grade 3 = 50—75% and grade 4 = 75—100% of segmental glomerular lesions. At least 30 glomeruli per group (n = 3—4) were analysed. Tubular damage was scored by calculating the percentage of tubules that display tubular cell necrosis, sloughing of tubular epithelial cells or loss of brush borders, cast formation and tubular dilatation as follows: 0 = none, 1 = ≤10%, 2 = 11—25%, 3 = 26—45%, 4 = 46—75% and 5 = ≥75% [29,30]. Ten random fields ($400 \times$ magnification) per mouse in each group were evaluated (n = 3—4). Details on grading assessment of renal tubular damage and glomerular injury are provided in Supplementary Figure 3. After

Picro-Sirius Red staining, eight sections from each mouse were analysed ($200\times$ magnification) to calculate the fibrotic area (n = 3—4), as previously described [31] using ImageJ software (National institutes of health (NIH), Bethesda, Maryland, USA).

2.7. Immunohistochemistry (IHC) analysis
The 10% formaldehyde-fixed and paraffin-embedded kidney tissue sections (5 μm-thick) were prepared. Briefly, the fixed kidney sections were deparaffinised, rehydrated and antigen-retrieved in sodium citrate buffer (10 mM, pH 6.0) for 20 min. The sections were blocked in 10% normal horse serum and incubated with a primary antibody against Wilms' tumour protein 1 (WT1) from Boster Biological Technology (Pleasanton, CA, USA) or LC3B from Sigma (St. Louis, MO, USA) overnight at 4 °C. The sections were incubated with a biotinylated secondary antibody (Vector Laboratories, Burlingame, CA, USA) for 1 h at room temperature. The sections were incubated in avidin-biotin-peroxidase complex solution (ABC solution; Vector Laboratories) for 30 min and developed using 3,3′-diaminobenzidine (DAB) Peroxidase Substrate Kit (Vector Laboratories). Then, the sections were counterstained with Mayer's haematoxylin and analysed using a CKX41 light microscope (Olympus). The number of stained nuclei was counted (equivalent to the number of podocytes) from 10 images of $200\times$ of HPF per kidney section from each group (n = 3). LC3B-positive cells were counted in the kidney sections stained by LC3B, from 10 images of $400\times$ magnification per section from each group (n = 3) using ImageJ software (NIH).

2.8. Immunofluorescence (IF) staining
Mouse kidneys were fixed in 10% formaldehyde and 5-μm-thick sections were deparaffinised, rehydrated and permeabilised in sodium citrate buffer (10 mM, pH 6.0) for 20 min. The sections were blocked in 10% normal goat serum and labelled with primary antibody of mouse monoclonal anti-p62 (Abcam) overnight at 4 °C. After washing, the slides were subsequently incubated with goat anti-mouse secondary antibody conjugated with Alexa Fluor® 594 for 1 h at room temperature and mounted with ProLong Gold Anti-fade mounting solution containing 4′,6-diamidino-2-phenylindole (DAPI, Thermo Fisher Scientific, Waltham, MA, USA), (n = 3). The images were captured using an Olympus Fluoview FV1000 confocal microscope and analysed by ImageJ (NIH).

2.9. Terminal deoxynucleotidyl transferase dUTP nick-end labelling (TUNEL) assay
TUNEL staining was performed to evaluate the degree of apoptosis using an In Situ Cell Death Fluorescein Detection Kit (Roche Molecular Biochemicals, Mannheim, Germany) according to the manufacturer's instructions. The images were captured using a Nikon Eclipse Ti—U microscope (Tokyo, Japan). The number of TUNEL-positive cells were counted from 5 images of $200\times$ magnification per section from each group (n = 3) using ImageJ software (NIH).

2.10. Western blot analysis
Kidney tissues were homogenised in ice-cold radio-immunoprecipitation assay (RIPA) buffer with protease inhibitors (Thermo Fisher Scientific), sonicated and incubated for 20 min on ice. After centrifugation, the supernatant was transferred to a clean tube, and the protein concentration was determined using a Pierce™ BCA Protein Assay Kit (Thermo Fisher Scientific). The protein lysates were separated using sodium dodecyl sulphate-polyacrylamide gel electrophoresis (SDS-PAGE), transferred to polyvinylidene difluoride (PVDF) membranes and blocked with 5% skim milk or 3% bovine serum albumin (BSA). The membranes were incubated with primary antibodies against SIRT-1, FOXO3a, p-FOXO3a, p-AKT, AKT, uncleaved caspase-3, cleaved caspase-3, uncleaved poly (ADP-ribose) polymerase 1 (PARP-1), cleaved PARP-1, autophagy-related gene 5 (ATG5), ATG12, Beclin-1, p-Beclin-1, light-chain 3B (LC3B) and p62 (Cell Signalling Technology, Danvers, MA, USA), p-ULK-1 and ULK-1 (Abcam) and β-actin (Sigma, St. Louis, MO, USA) in the blocking solution at 4 °C overnight. Next, the membranes were incubated with the appropriate horseradish peroxidase (HRP)-conjugated secondary antibodies (Bio-Rad, Hercules, CA, USA) at room temperature for 1 h and then visualised with the ECL substrate (Bio-Rad). The ChemiDoc XRS + System (Bio-Rad) was used to evaluate the density of protein bands, and relative protein levels were quantified using Image Lab™ software (Bio-Rad). Detailed information on antibodies is shown in Table 2.

2.11. Quantitative real-time polymerase chain reaction (PCR) analysis
The total RNA was extracted with Trizol (Invitrogen, Carlsbad, CA, USA) and converted into cDNA using the RevertAid Reverse Transcription System (Thermo Fisher Scientific) according to the manufacturer's protocol. Real-time PCR analysis was performed with a CFX Connect real-time PCR System using iQ SYBR Green Supermix (Bio-Rad). Real-time PCR analysis was performed with initial denaturation at 94 °C for 5 min, and the cycling conditions were 45 cycles of 10 s at 95 °C, 10 s at 60 °C and 30 s at 72 °C. Relative mRNA levels were normalised to those of glyceraldehyde 3-phosphate dehydrogenase (GAPDH). The primer sequences are listed in Table 1.

2.12. Statistical analysis
Statistical significance was determined using one-way analysis of variance (ANOVA), followed by Bonferroni's multiple comparisons for multiple group or unpaired two-tailed Student's t-test to compare two groups (GraphPad Prism 7 Software, v.7.00, La Jolla, CA, USA). Data were expressed as the mean ± SEM. $*p < 0.05$, $**p < 0.01$, $***p < 0.001$ vs WT control mice; and $^{\#}p < 0.05$, $^{\#\#}p < 0.01$, $^{\#\#\#}p < 0.001$ vs WT DN mice.

3. RESULTS

3.1. P2Y2R deficiency reduced albuminuria and attenuated renal dysfunction in DN
To decipher the role of P2Y2R on kidney function in DN, we examined the effect of P2Y2R deficiency using P2Y2R global KO mice on the

Table 1 — Primer sequences used for real-time PCR analysis in this study.

Gene	Forward primers (5′-3′)	Reverse primers (3′-5′):
ATG5	GATGTGCTTCGAGATGTGTGGTTTG	CAACGTCAAATAGCTGACTCTTGGC
ATG7	CGCTTGACGTTGGAGTTCAGTG	GTGTTGTGCAGGGTTCCCATG
ATG12	GGAAGATTCAGAGGTTGTGCTGCA	GAGTGTCTCCTACAGCCTTCAGC
ATG14	AAGTGCGTCCAGAGCGGTGATTTC	CCATCTCAACTGATCTGTAAGCCGC
Beclin-1	GTCTAAGGCGTCCAGCAGCAC	TGGGCGTGTGGTAAGTAATGGAGC
BNIP3	CTGCACTTCAGCAATGGCAATGG	GCTACTTCGTCCAGATTCATGCTGG
FOXO3a	CTGTCCTATGCCGACCTGATCAC	CATTCTGAACGCGCATGAAGCG
GAPDH	GTGGCAAAGTGGAGATTGTTG	TTGACTGTGCCGTTGAATTTG
KIM-1	GAGAGTGACAGTGGTCTGTATTG	CCTTGTAGTTGTGGGTCTTCTT
LC3B	CAAGATAATCAGACGGCGCTTGCA	CATTGCTGTCCCGAATGTCTCCTG
NGAL	CACCACGGACTACAACCAGTTCGC	TCAGTTGTCAATGCATTGGTCGGTG
NPHS1	GGTGGAAGGGTCGACAGTTAAGCT	CTCGTACTCCGCATCATCGCTGA
NPHS2	CCGTCTCCAGACCTTGGAAATACC	GGACACATGGGCTAGACTGCTTAG
P2Y1R	AGCATCTTGTTCCTCACCTGCATC	TCATTGGACGTGGTGTCATAGCAG
P2Y2R	GTGCTCTACTTCGTCACCACCAG	CCATAAGCACGTAACAGACCAGGA
P2Y6R	GCACTGGCGGACCTGATGTATG	GGATGCTGCCATGTAGATTGGCA
SIRT-1	GCACCGATCCTCGAACAAT	ATCTGCCACAGCGTCATATC
ULK-1	CTCGCAAGGACCTGATTGGACAC	CATTTGACGGCCACCTCCAGGT

Table 2 — Antibodies used in this study.

Antibody	Source	Catalog No.	Host	Dilution
LC3B	Cell signaling	#2775S	Mouse	34 ng/ml (WB)
LC3B	Sigma	#L7543	Rabbit	10 µg/ml (IHC)
Caspase 3	Cell signaling	#9662	Rabbit	98 ng/ml (WB)
PARP-1	Cell signaling	#9542	Rabbit	195.2 ng/ml (WB)
ATG 5	Cell signaling	#12994	Rabbit	220 ng/ml (WB)
ATG12	Cell signaling	#4180	Rabbit	40 ng/ml (WB)
Beclin-1	Cell signaling	#3495	Rabbit	111 ng/ml (WB)
p-Beclin-1^{Ser15}	Cell signaling	# 84966	Rabbit	1.018 µg/ml (WB)
p62	Cell signaling	#5114	Rabbit	18.1 ng/ml (WB)
p62	Abcam	#ab56416	Mouse	10 µg/ml (IF)
SIRT-1	Cell signaling	#9475	Rabbit	42 ng/ml (WB)
AKT	Cell signaling	#9272	Rabbit	34 ng/ml (WB)
p-AKT^{Ser473}	Cell signaling	#9271	Rabbit	20 ng/ml (WB)
FOXO3a	Cell signaling	#9464	Rabbit	131 ng/ml (WB)
p-FOXO3a^{Ser253}	Cell signaling	#9466	Rabbit	1.816 µg/ml (WB)
ULK-1	Abcam	#ab167139	Rabbit	1 ng/ml (WB)
p-ULK-1^{Ser757}	Abcam	#ab229909	mouse	1.19 µg/ml (WB)
Wilms Tumor-1 (WT1)	Boster Biological Technology	#M00199-1	Rabbit	1 µg/ml (IHC)
Goat anti-rabbit HRP conjugate	Bio-rad	#170-6515	Rabbit	1:5000 (WB)
Goat anti-mouse HRP conjugate	Bio-rad	#170-6516	mouse	1:5000 (WB)
β-Actin	Sigma	#A5441-2ML	mouse	1:20,000 (WB)
Goat anti-mouse IgG-Alexa Fluor 594	Abcam	#ab150116	Mouse	2 µg/ml (IF)

pathogenesis of DN. As shown in Figure 1A, DN was induced by STZ injection to the WT or P2Y2R KO mice after 3 weeks of UNx and HFD feeding and then sacrificed at 6 weeks after STZ injection. The control mice were fed with a normal chow diet (NCD). The efficiency of P2Y2R KO was confirmed by real-time PCR analysis (Figure 1B) by showing the absence of P2Y2R expression in KO mice. To investigate the development of DN, critical renal parameters were measured. P2Y2R KO DN mice exhibited a significant reduction in plasma creatinine, BUN and blood glucose levels compared to WT DN mice (Figure 1C, D, E). KO DN mice had a significantly reduced urine albumin/creatinine ratio (UACR) and excreted urine volume (Figure 1F, G) compared to WT DN mice. Additionally, relative kidney weight was reduced (Figure 1H) in KO DN mice; however, no differences in body weight were found between WT and KO DN mice (Supplementary Fig. 1A). The extracellular ATP, a P2Y2R ligand, was increased in WT DN compared to WT controls (Supplementary Fig. 1B), which suggests the activation of P2Y2R signalling in the pathogenesis of DN. Moreover, P2Y2R KO enhanced the expression of P2Y1R and P2Y6R compared WT DN mice (Supplementary Fig. 1C), which may be a compensatory response to the P2Y2R deficiency. The results indicate that P2Y2R deficiency improves renal filtration function and attenuates DN-induced renal dysfunction.

3.2. P2Y2R deficiency attenuated podocyte loss and glomerular injury in DN

Podocyte damage is a key characteristic in the pathogenesis of DN [32]. To investigate the podocyte integrity and function in the diabetic mice, we examined the specific podocyte gene expression by real-time PCR analysis and revealed that P2Y2R deficiency increased the gene expression levels of Nphs-1 (nephrin) and Nphs-2 (podocin), which were downregulated in WT DN mice (Figure 2A). We also examined the WT1, a podocyte marker, by IHC staining. The podocyte number was significantly decreased in WT DN mice compared to WT controls, clearly indicating significant podocyte damage. Importantly, P2Y2R deficiency restored the number of podocytes in diabetic kidneys

(Figure 2B). We next determined the extent of glomerular lesions by PAS staining, and histological analysis showed that glomerular injury was significantly reduced in KO DN mice compared to WT DN mice (Figure 2C). These results indicate that P2Y2R promotes substantial loss of podocytes and glomerular injury in DN.

3.3. P2Y2R deficiency reduced renal tubular injury and interstitial fibrosis in DN

Recent studies have characterised KIM-1 (kidney injury molecule-1) and NGAL (neutrophil gelatinase-associated lipocalin) as potential and sensitive biomarkers of renal tubular injury in acute kidney injury (AKI) that are the key drivers for CKD [33,34]. To assess the effect of P2Y2R deficiency on tubular damage, the expression of these biomarkers was determined by real-time PCR analysis. The mRNA levels of KIM-1 and NGAL were significantly upregulated in WT DN mice compared to WT control mice but reduced in KO DN mice (Figure 3A). The tubular damage was further confirmed by PAS staining of renal tubules in renal cortex compartments, where WT DN mice increased renal tubular injury (damaged tubules are indicated by black arrows in Figure 3B). WT DN mice also showed a significant induction of interstitial fibrosis determined by Picro-Sirius Red staining (Figure 3C). Renal tubular damage and interstitial fibrosis were both reduced in KO DN mice compared to WT DN mice, indicating consistently that P2Y2R deficiency attenuates renal dysfunction and delays the development of DN.

3.4. P2Y2R deficiency reduced renal apoptosis in DN

Renal apoptosis plays an active role in renal tubular damage and progression of DN in experimental murine models and human patients [35,36]. To investigate the effect of P2Y2R deficiency on renal apoptosis induced by DN, we performed TUNEL staining to evaluate the occurrence and extent of apoptosis. The results showed a significant increase in the number of TUNEL-positive cells in WT DN mice, which was decreased in KO DN mice (Figure 4A). Next, we conducted the
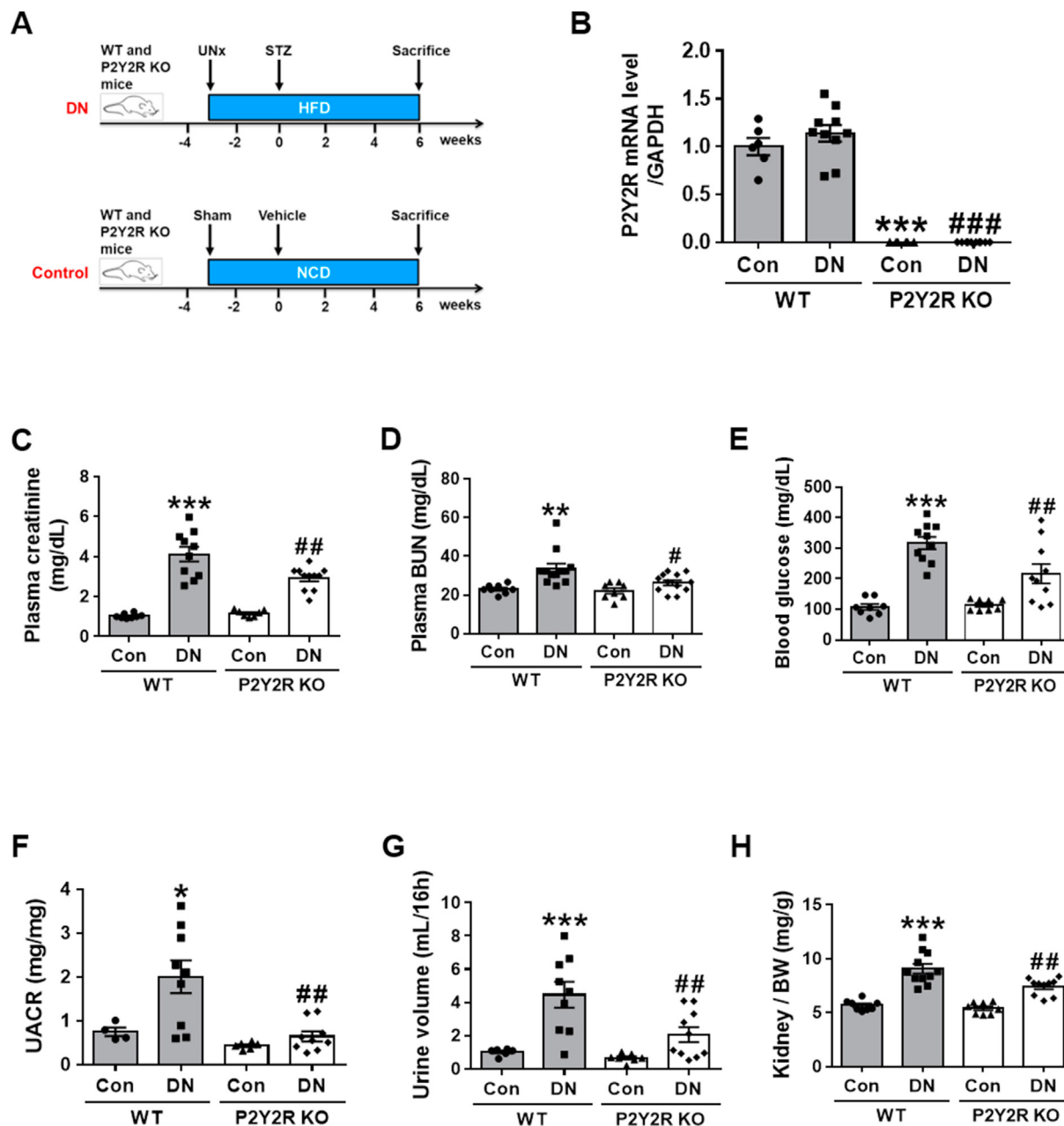
Figure 1: P2Y2R KO mice decrease albuminuria and renal dysfunction induced by DN. DN animal model was generated by STZ injection (100 mg/kg) to the WT or P2Y2R KO mice after 3 weeks of UNx and HFD feeding and then sacrificed at 6 weeks post-STZ injection. The control mice were fed with a normal chow diet (NCD). Blood and urine samples were collected from WT and P2Y2R KO control (n = 8) or DN (n = 12−14). (A) Schematic representation of experimental design. (B) Expression of endogenous P2Y2R in kidney tissues from WT and KO mice (n = 3−5). (C, D, E) Plasma creatinine, blood urea nitrogen (BUN) and blood glucose levels were measured, respectively (control n = 8, DN n = 14). (F, G, H) Urine albumin/creatinine ratio (UACR), urine volume (mL/16 h), and kidney/body weight (BW) ratio at 6 weeks post-STZ injection (control n = 8, DN n = 14). Data are presented as mean ± SEM. One-way ANOVA was used for statistical analysis followed by Bonferroni's multiple comparisons test. $*p < 0.05$, $**p < 0.01$, $***p < 0.001$ vs WT control mice; and $^#p < 0.05$, $^{##}p < 0.01$, $^{###}p < 0.001$ vs WT DN mice.

western blot analysis to assess cleavage of caspase-3 and PARP-1. The cleavage of caspase-3 and PARP-1 was significantly increased in WT DN mice, while P2Y2R deficiency reversed renal apoptosis induced by DN. These data indicate that P2Y2R deficiency attenuates renal dysfunction and delays the development of DN.

3.5. P2Y2R deficiency increased autophagy response in DN

Dysregulated autophagy plays a detrimental role in the pathogenesis of DN [1], and pharmacological activation of autophagy was reported to exert a renoprotective effect in DN, as previously shown in our work and other studies [25,37]. To determine autophagy activity in DN, we examined the expression of autophagy-related proteins (ATGs), Beclin-1 and autophagy flux markers (LC3B and p62) in the diabetic kidneys. P2Y2R deficiency significantly enhanced the expression of ATG5, ATG12 and Beclin-1 and improved autophagy dynamics as determined by the increased LC3B-II and decreased p62 levels in DN mice (Figure 5A). Additionally, we examined the LC3B expression by IHC staining and found a significant increase of LC3B-positive cells in KO DN mice
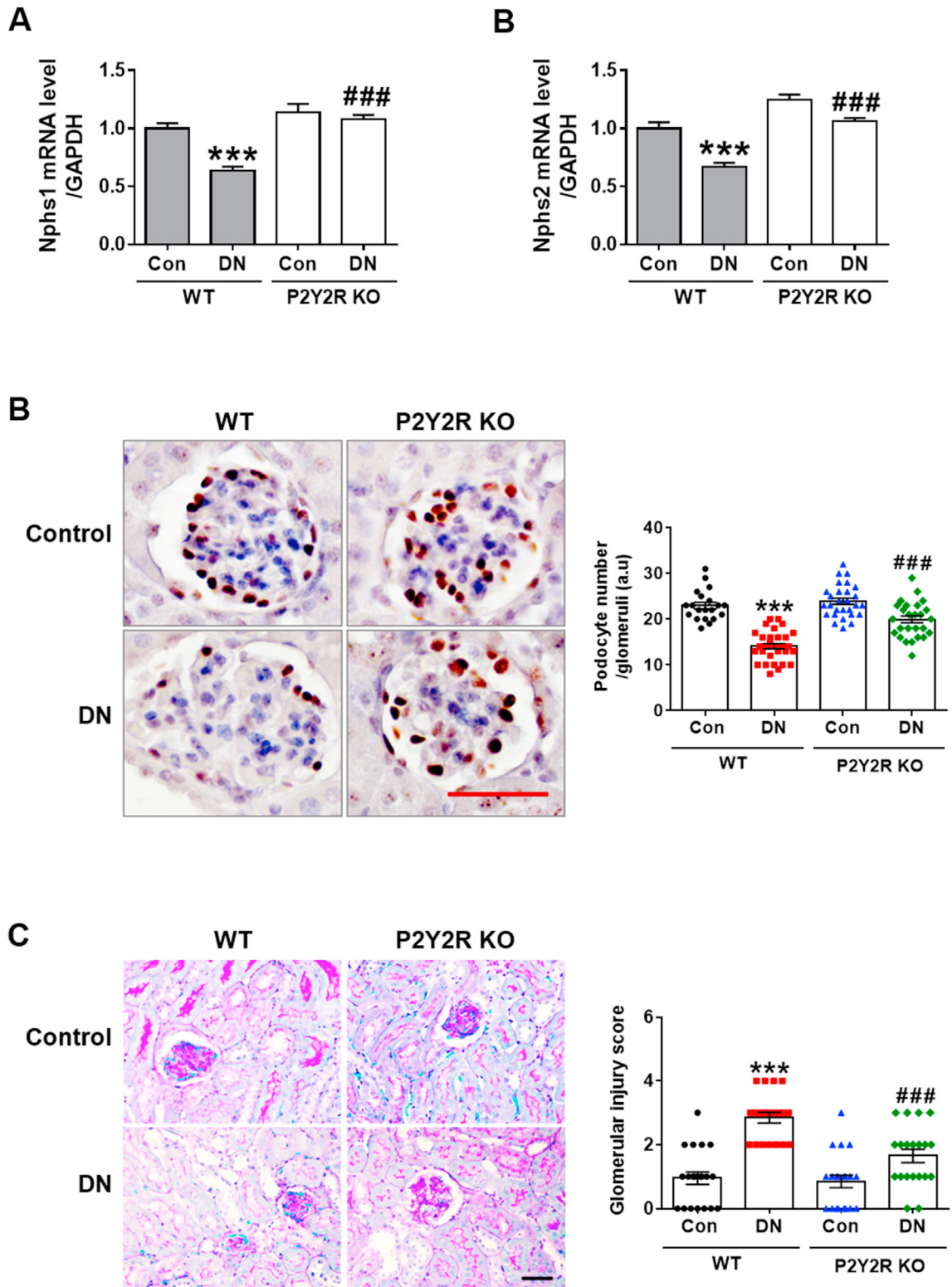
Figure 2: P2Y2R deficiency protects against podocyte loss and glomerular injury in DN. (A) Relative mRNA levels of Nphs1 (nephrin) and Nphs2 (podocin) were determined by real-time PCR analysis (n = 3–5). (B) Localisation of WT1, a podocyte marker, was analysed by immunohistochemistry, and representative images are shown. The number of stained podocytes per glomeruli was counted by using ImageJ software (n = 3). (C) Kidney sections were stained with PAS staining and glomerular morphological changes were scored as described in the method section (n = 3). Data are presented as mean ± SEM. One-way ANOVA was used for statistical analysis followed by Bonferroni's multiple comparisons test. ***p < 0.001 vs WT control mice; and ###p < 0.001 vs WT DN mice. Scale bar, 50 μm.
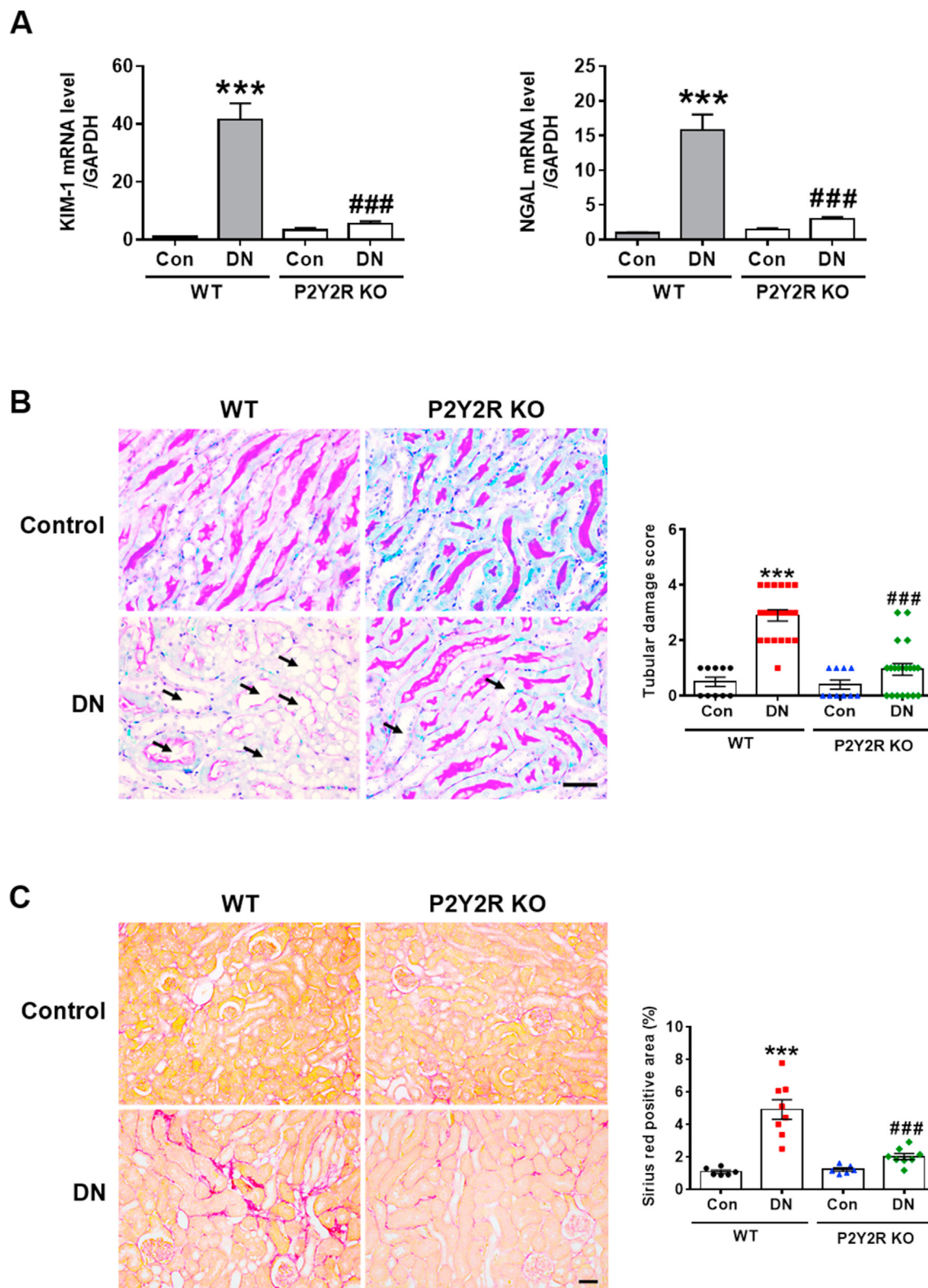
Figure 3: P2Y2R KO mice reduce renal tubular injury and interstitial fibrosis in DN. (A) Kidney injury molecule-1 (KIM-1) and neutrophil gelatinase-associated lipocalin (NGAL), the specific biomarkers for renal tubular damage, were assessed by real-time PCR analysis (n = 3−5). (B) Renal tubular damage was analysed by PAS staining, the representative images were shown, and the tubular damage scores were evaluated (black arrows indicate damaged renal tubules), (n = 3). (C) Picro-Sirius Red staining was performed in kidney sections and fibrotic area was presented as percentages (%) by using ImageJ software (n = 3). Data are presented as mean ± SEM. One-way ANOVA was used for statistical analysis followed by Bonferroni's multiple comparisons test. ***$p < 0.001$ vs WT control mice; and ###$p < 0.001$ vs WT DN mice. Scale bar, 50 μm.
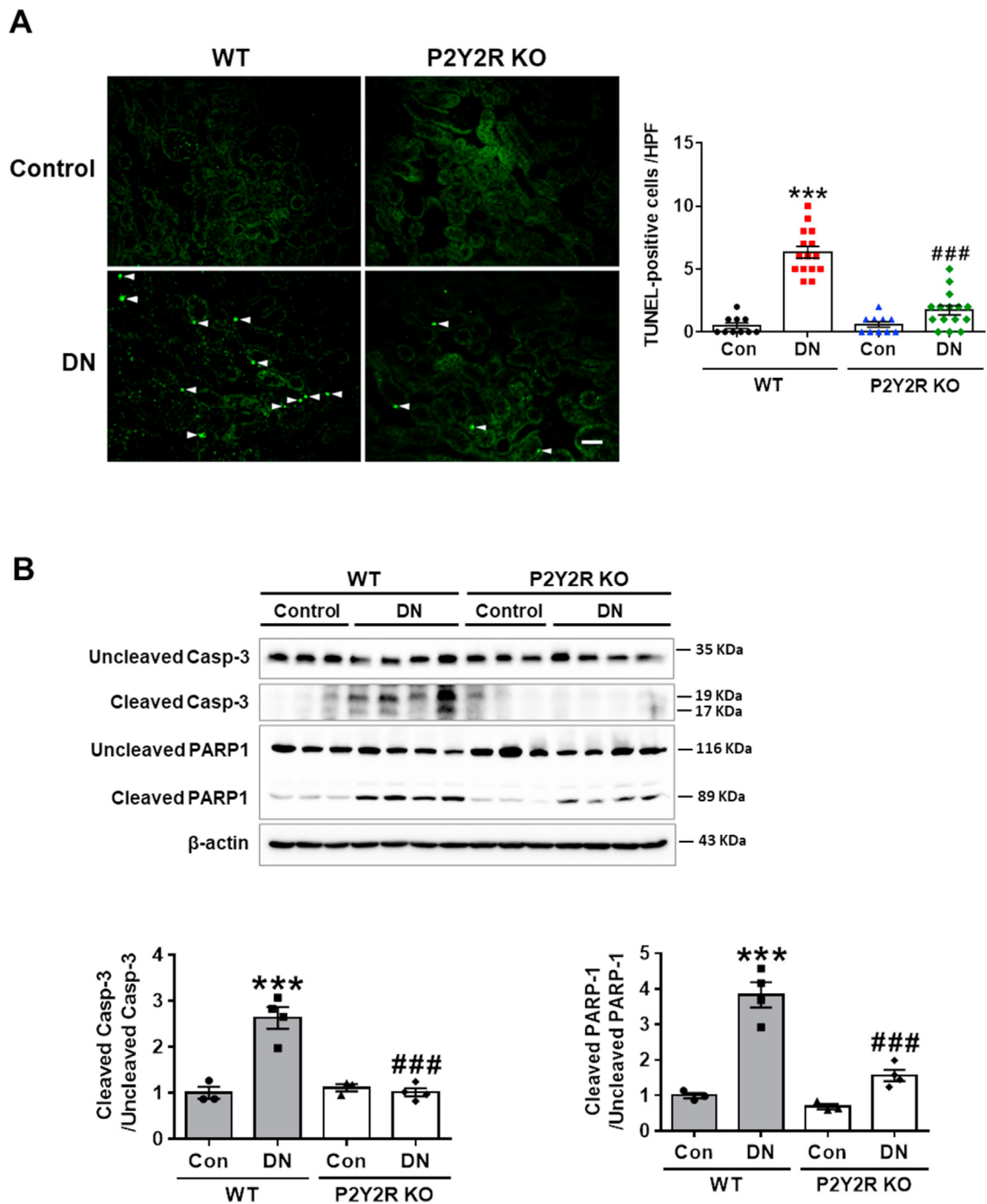
A

B

Figure 4: P2Y2R deficiency attenuates renal apoptosis in DN. (A) Representative images of TUNEL staining that were processed in the kidney sections to determine DN-induced renal apoptosis. The number of TUNEL-positive cells/HPF was counted to present the severity of apoptosis (n = 3). (B) The extent of apoptosis was further determined by caspase-3 and PARP-1 cleavage in kidney tissue lysates using western blot analysis, and the quantitative values are shown (n = 3–4). Data are presented as mean ± SEM. One-way ANOVA was used for statistical analysis followed by Bonferroni's multiple comparisons test. ***$p < 0.001$ vs WT control mice and ###$p < 0.001$ vs WT DN mice. Scale bar, 100 μm.

compared to WT DN mice (Supplementary Fig. 2). Consistently, real-time PCR analysis revealed that autophagy-related gene transcripts were downregulated in WT DN mice, and this reduction was markedly blunted in KO DN mice (Figure 5B). We also performed the immunofluorescence staining of p62; impaired autophagy is evidenced by cytoplasmic accumulation of p62, a substrate of autophagy-lysosomal degradation pathway. WT DN mice showed a significant cytoplasmic accumulation of p62 compared to WT control, and the levels were decreased in KO DN mice (Figure 5C). These data indicate that P2Y2R deficiency enhances autophagy and possibly ameliorates the progression of DN.
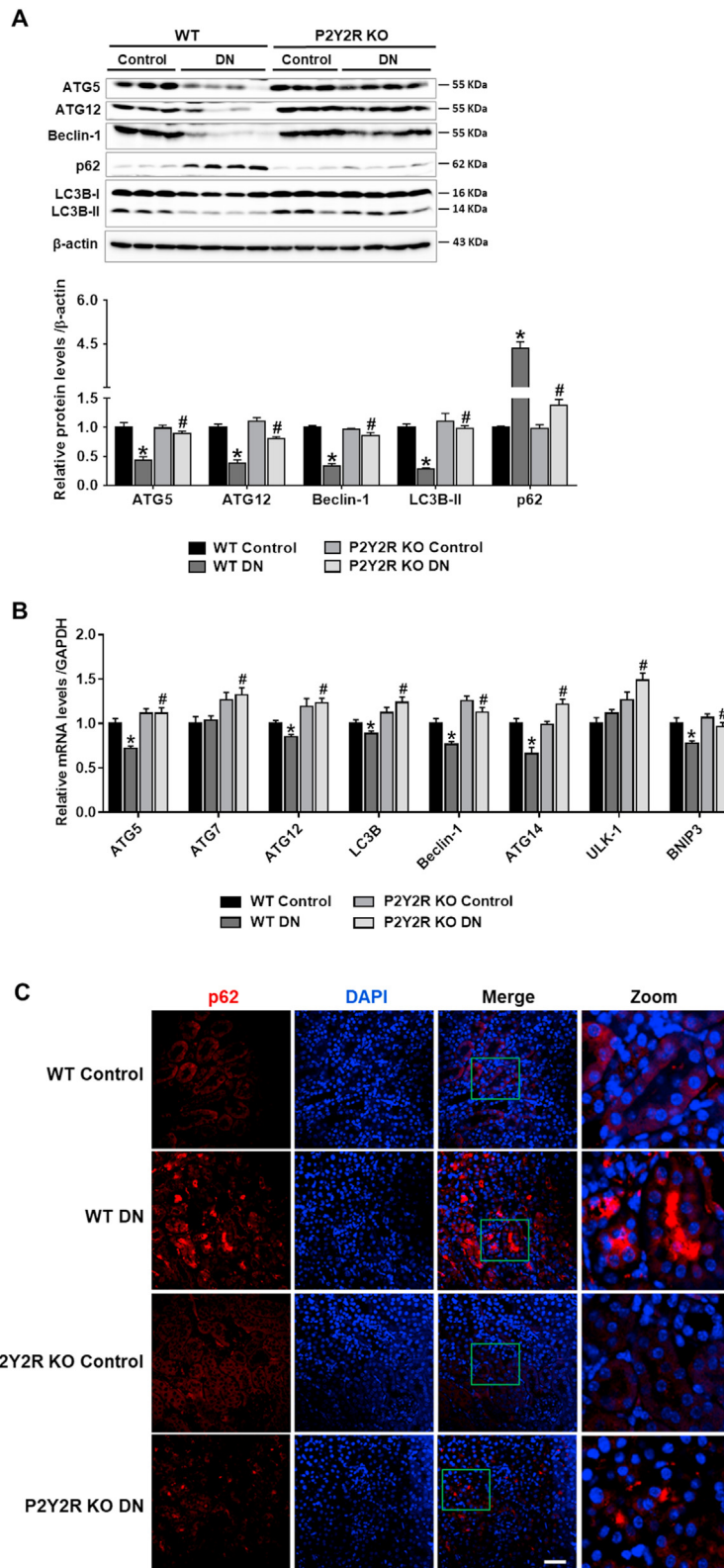
Figure 5: P2Y2R deficiency enhances autophagy signalling in DN. (A) Kidney tissues were lysed to perform western blot analysis, and the levels of autophagy proteins (ATG5, ATG12, Beclin-1, p62 and LC3B) and β-actin, as a loading control, were examined. Quantitative analysis of each protein was shown (n = 3−4). (B) Autophagy-related gene transcripts were determined by real-time PCR analysis. Relative mRNA expression was normalised to that of GAPDH (n = 3−5). (C) Representative images of immunofluorescence staining of p62 (red) were assessed by confocal microscopy (n = 3). Data are presented as mean ± SEM. One-way ANOVA was used for statistical analysis followed by Bonferroni's multiple comparisons test. *$p < 0.05$ vs WT control mice; and #$p < 0.05$ vs WT DN mice. Scale bar, 20 μm.
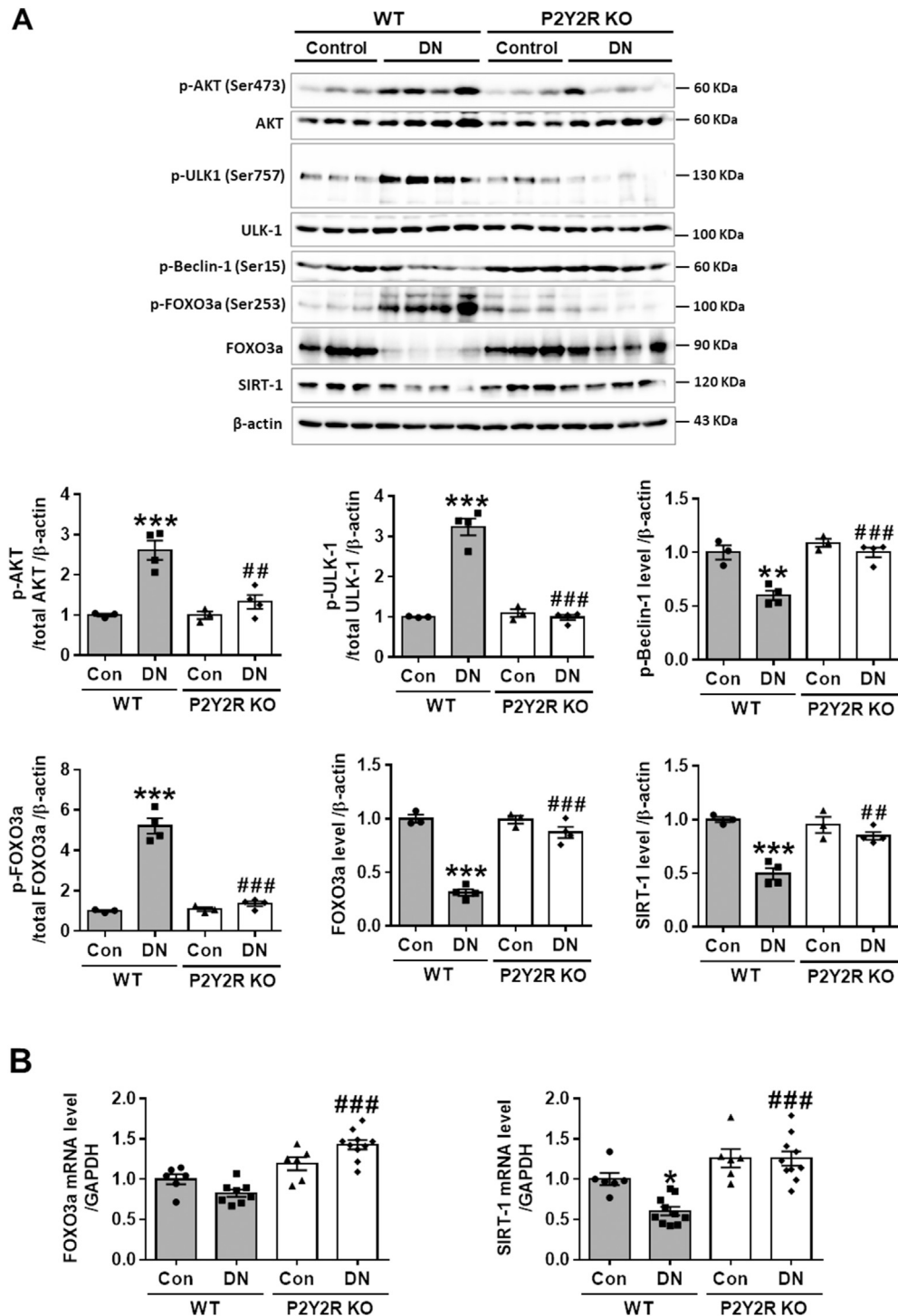
Figure 6: P2Y2R deficiency alters the protein levels of p-AKT, p-FOXO3a, p-ULK-1, p-Beclin-1 and SIRT-1 in DN. (A) The protein expression levels of p-AKT, p-FOXO3a, p-ULK-1, p-Beclin-1, SIRT-1 and β-actin, as a loading control, were examined by for western blot analysis in kidney tissue lysates. Quantitative analysis of each protein level is shown (n = 3–4). (B) Relative mRNA levels of FOXO3a and SIRT-1 were determined by real-time PCR analysis in the kidney tissues. Relative mRNA expression was normalised to that of GAPDH (n = 3–5). Data are presented as mean ± SEM. One-way ANOVA was used for statistical analysis followed by Bonferroni's multiple comparisons test. *p < 0.05, **p < 0.01, ***p < 0.001 vs WT control mice; and ##p < 0.01, ###p < 0.001 vs WT DN mice.

3.6. P2Y2R deficiency decreased AKT/FOXO3a signalling that induces autophagy dysfunction

To determine the potential mechanism of P2Y2R in regulation of autophagy in DN mice, the expression of p-AKT, p-FOXO3a, p-ULK1, p-Beclin-1 and SIRT-1 were evaluated by western blot analysis. FOXO3a plays a critical role in regulating autophagy in various diseases; in response to stress or pathological conditions, FOXO3a is phosphorylated by AKT and is retained in the cytosol, thereby blocking its

transcriptional activity [1,37—39]. Consistently, we found that the levels of phosphorylation in AKT (Ser473) and its substrate FOXO3a (Ser253) were significantly increased in WT DN mice compared to WT control mice, while the levels were decreased in KO DN mice (Figure 6A). Inhibitory phosphorylation of ULK-1 (Ser757) has been reported to decreased the phosphorylation of Beclin-1 (Ser15) that promotes autophagy initiation by phagophore formation [40]. We examined whether the phosphorylation of AKT could increase the inhibitory kinase activity of ULK-1 that interacts with the Beclin-1 and ATG14 complex for initiating autophagy. The results showed that p-AKT (Ser473) levels were positively correlated with p-ULK-1 (Ser757) levels and negatively correlated with p-Beclin-1 (Ser15) levels in WT DN mice, while P2Y2R deficiency reversed these changes (Figure 6A). Furthermore, SIRT-1 has been assigned to a renoprotective effect by modulating autophagy response through deacetylation of multiple transcription factors including FOXO3a in DN [11,37]. Because SIRT-1 and FOXO3a signalling play a key role in autophagy induction [1,38,40], we examined the effect of P2Y2R deficiency on SIRT-1 and FOXO3a expression in DN. The protein and mRNA levels of SIRT-1 and FOXO3a were significantly downregulated in WT DN mice, while the levels were restored in KO DN mice (Figure 6A, B). The reduced p-

FOXO3a (Ser253) and increased FOXO-3a expression in KO DN mice indicate that P2Y2R deficiency activates the transcription of FOXO3a and promotes induction of autophagy genes. Taken together, P2Y2R activation impairs the FOXO3a and SIRT-1-mediated autophagy function and contributes to the development of DN. Conversely, P2Y2R deficiency preserves autophagy activity and ameliorates the DN pathology.

3.7. Schematic mechanism of P2Y2R in the development of DN via AKT/FOXO3a and SIRT-1 signalling

Hyperglycaemia and extracellular ATP activate P2Y2R, which induces autophagy dysfunction, resulting in renal apoptosis, glomerular injury, and interstitial fibrosis, ultimately promoting DN. Mechanistically, the strong upregulation of AKT phosphorylation plays a detrimental role by increasing apoptosis, inactivating autophagy initiation through the ULK-1 and Beclin-1 pathways, and negatively regulating the FOXO3a-mediated induction of autophagy-related genes. KO DN mice exhibit decreased AKT phosphorylation and increased FOXO3a and SIRT-1 expression. Therefore, P2Y2R deficiency restores autophagy response through AKT, FOXO3a and SIRT-1 signalling pathways, thus attenuating the pathological changes of DN (Figure 7).
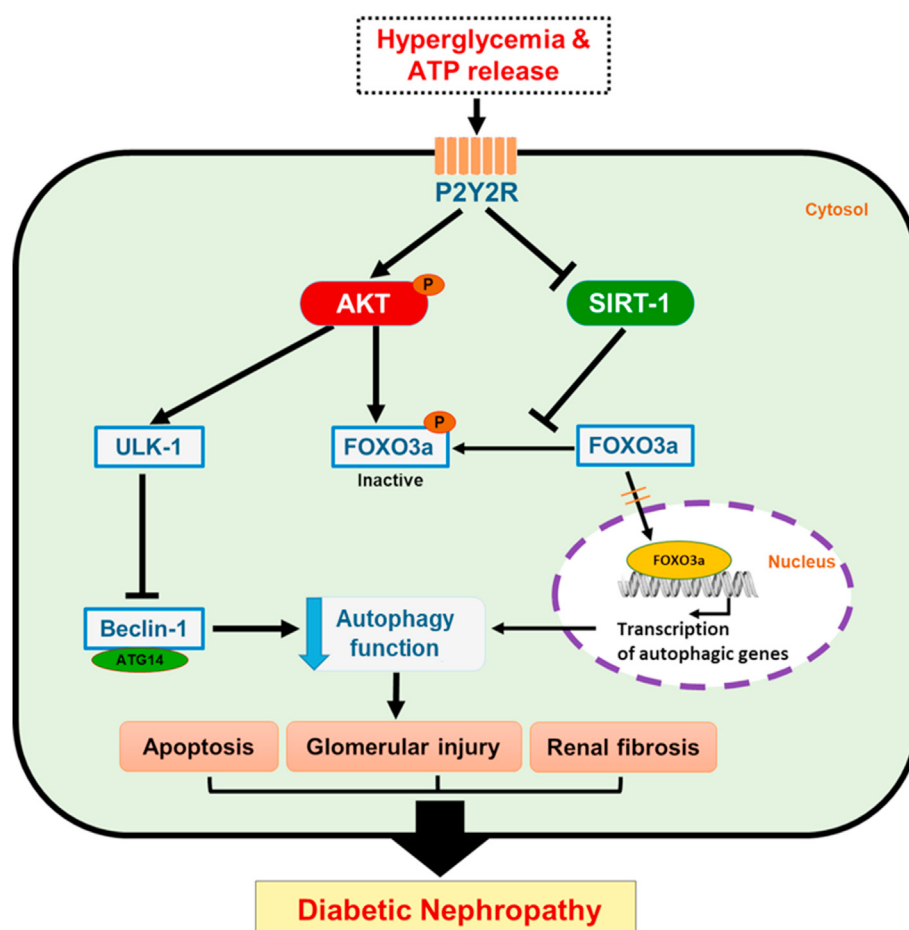

Figure 7: Schematic molecular mechanism of P2Y2R in the development of DN. P2Y2R activation via hyperglycaemia and extracellular ATP increases AKT phosphorylation, and the increased AKT activity promotes an inhibitory ULK-1 phosphorylation that downregulates autophagy through inhibition of Beclin-1 and ATG14 complex required for phagophore formation, resulting in renal apoptosis, glomerular injury and interstitial fibrosis. In addition, the increased phosphorylation of FOXO3a by AKT activity and the inhibited SIRT-1 activity reduced autophagy response by downregulating transcription of autophagy genes. Conversely, P2Y2R knockout mice have reduced AKT phosphorylation and increased FOXO3a and SIRT-1 expression to rescue autophagy response and attenuate the progression of DN.

4. DISCUSSION

DN is a severe complication of diabetes, which occurs in 20—40% of all diabetic patients and therefore affects hundreds of millions of people worldwide [1,11]. Although many studies suggest the pathogenic mechanisms and appropriate treatments for DN, it remains a substantial clinical problem. Thus, new therapeutic targets underlying in the pathogenesis of DN are urgently needed. In this study, we investigated the role of P2Y2R in the development of DN in mice and found P2Y2R to be a potential pathogenic mediator of DN by inhibiting autophagy, based on the following results. First, P2Y2 deficiency reduced kidney functional damage, such as massive albuminuria and increased plasma creatinine and BUN levels induced by DN. Second, P2Y2R deficiency protected kidneys from podocyte loss, glomerular and tubular injury, interstitial fibrosis, and renal apoptosis induced by DN. Third, P2Y2R deficiency blocked the development of DN by activating autophagy signalling. Mechanistically, P2Y2R deficiency inhibited AKT activation, which regulates autophagy induction negatively through the ULK-1 and Beclin-1 pathways, and simultaneously upregulated SIRT-1/FOXO3a pathway, which increases the transcription of autophagy genes.

The extracellular ATP exerts various cellular responses, including inflammation, tissue damage, cell proliferation and allograft through membrane-anchored ionotropic P2XRs and metabotropic P2YRs; these receptors modulate normal kidney function but are also implicated in the development of renal diseases, such as diabetes, hypertension, and polycystic kidney disease (PKD), although precise mechanisms are not fully understood [14,41]. A comparative study of P2XRs and P2YRs reported a differential modulation of extracellular matrix and transforming growth factor (TGF)-β production in rat mesangial cells under hyperglycaemia during the development of DN [20]. P2X4R signalling has been shown to mediate high-glucose activation of the NLRP3 inflammasome and interleukin (IL)-1β and IL-18 release and cause tubulointerstitial inflammation in patients with DN [42]. Other studies also reported that P2X4R and P2X7R are upregulated, and tubular P2X4R colocalises with NLRP3, IL-1β and IL-18 expression in patients of type 2 diabetes and DN [42,43]. An increase in P2X7R expression was observed in glomerulonephritis, and P2X7R deficiency was shown to be protective, displaying reduction in glomerular damage, proteinuria and serum creatinine [44,45]. In a rat model of PKD, the renal expression of P2X7R, P2Y2R and P2Y6R was increased, and the use of inhibitors reduced cyst growth [46,47]. The antagonists or inhibitors of P2X1R, P2X7R and P2Y2R also reduced arterial blood pressure and vascular resistance via salt and water regulation, suggesting potential benefits in hypertension [15,48,49]. Therefore, targeting eATP and purinergic receptors may be a clinically important therapeutic strategy for various renal diseases.

Here, we investigated whether P2Y2R has a pathogenic or protective role during the development of DN in mice and performed a mechanistic study. P2Y2R is expressed in the glomerular, mesangial, podocyte and tubular cells in the kidney. The activation of P2Y2R is associated with various renal cellular responses, including inflammation, apoptosis, chloride secretion, cell proliferation and vascular remodelling [13—17]. Blocking P2Y2R using suramin (a non-selective P2Y receptor antagonist) attenuated proteinuria, glomerular and tubulointerstitial damage and improved renal function in a rat model of CKD [50]. Indeed, Rennert et al. reported that P2Y2R deficiency is renoprotective in a mouse model of antibody-mediated crescentic glomerulonephritis [24]. However, the precise molecular mechanisms of P2Y2R in the pathogenesis of DN remains unknown.

P2Y2R expression levels were not statistically different between WT control and DN mice. However, extracellular ATP, a P2Y2R ligand, was significantly increased in WT DN compared to WT control. This finding suggests that an increase of extracellular ATP might activate P2Y2R and exerts its pathologic function in DN. This is supported by a previous study in which the hydrolysis of extracellular ATP by ectonucleotide triphosphate diphosphorylase 1 (ENTOD1), known as CD39, was found to prevent chronic glomerular injury in DN [51]. Extracellular ATP and UTP have short half-lives due to rapid catabolism, and their immediate breakdown products, ADP and UDP, are potent agonists of P2Y1R and P2Y6R, respectively. CD39 further hydrolyses into AMP (or UMP) and eventually CD73, ecto-5′-nucleotidase (Ecto5′NTase), dephosphorylates into adenosine (or uridine) [12]. In our study, P2Y2R KO mice showed an increase of P2Y1R and P2Y6R expression in a DN mouse model, which may be a compensatory response to the P2Y2R deficiency. Thus, further studies may be required to access any functional crosstalk of P2Y2R and P2Y1R or P2Y6R and differential expression of CD39 or CD73 in the progression of DN and other renal diseases.

Here, we demonstrated that P2Y2R deficiency protected kidneys from podocyte loss and glomerular injury, which are key characteristics in the development of proteinuria and the progression to DN, especially in the early stages [3,32]. As previously shown, proximal tubule injury induces maladaptive repair, giving rise to interstitial fibrosis, tubular atrophy and potentially secondary glomerulosclerosis; which are critical features in the pathogenesis of AKI [52] and DN [53,54]. Similarly, we demonstrated that P2Y2R deficiency attenuated renal tubular damage, as assessed by KIM-1 and NGAL (specific biomarkers of renal tubular injury [33]), and reduced interstitial fibrosis determined by collagen deposition. In addition, we found that P2Y2R deficiency decreased renal apoptosis, as apoptosis plays an active role in renal tubular damage that potentiates the DN complications [55]. Thus, the results support our hypothesis that P2Y2R acts as a potential pathogenic mediator of DN, and its inhibition blocks the progression of DN. Autophagy serves as an essential mechanism to maintain homeostasis of glomerular and renal tubular cells in human health and diseases [56]. Autophagy impairment has been implicated in the pathogenesis of DN [1,57]. Importantly, emerging evidence suggests that targeting the autophagy pathway to activate and restore the autophagy activity is renoprotective against DN [8,58,59]. In this regard, we demonstrated that P2Y2R deficiency significantly enhanced autophagy activity, which was altered in DN, by increasing autophagy flux (LC3B-II and p62) and expression of other autophagy-related proteins (ATG5, ATG12, Beclin-1). The improved autophagy observed in KO DN mice is associated with survival mechanism by suppressing the accumulation of p62, a marker of autophagy impairment. The enhanced autophagy activity in P2Y2R deficiency may play an important role in the clearance of autophagic substrates and a delay in the progression of DN.

We explored the molecular mechanisms of P2Y2R deficiency that confers a renoprotective effect against DN and found altered expression of p-AKT, p-FOXO3a, p-ULK1, p-Beclin-1 and SIRT-1 that mediate autophagy signalling in WT and KO DN mice. In literature, PI3K/AKT signalling plays a central role in glucose homeostasis, lipid metabolism and cell proliferation and survival [60]. The alteration of the PI3K/AKT signalling pathway leads to insulin resistance during the development of obesity and type 2 diabetes [60]. Extracellular ATP activates P2Y2R, which increases AKT activity in thick ascending limbs (TAL) of the nephron; importantly, suramin significantly blocks the AKT signalling pathway and prevents TAL dysfunction [61]. Our study found that P2Y2R signalling activates the AKT signalling pathway, which plays a detrimental role in the pathogenesis of DN by inhibiting the autophagy

pathway. Conversely, in KO mice, Akt signalling is abolished, and autophagy inhibition is relieved.

In response to stress or pathologic conditions, FOXO3a is phosphorylated by AKT and retained in the cytosol, resulting in the suppression of transcriptional activity [1,37—39]. Consistently, our study showed that activation of AKT increased the FOXO3a phosphorylation and suppressed FOXO3a-mediated transcriptional activity required for autophagy induction, facilitating the pathogenesis of DN. Importantly, P2Y2R deficiency downregulated AKT activity, thus enhancing the expression of autophagy-related genes and improved autophagy flux as well. Previously, pharmacological inhibition of PI3K/AKT signalling was found to ameliorate albuminuria, renal tubular injury, and epithelial-to-mesenchymal transition during progression to renal fibrosis in a rat model of diabetic kidney disease [62]. Autophagy was shown to attenuate tubulointerstitial fibrosis through regulating TGF-β and NLRP3 inflammasomes [63]. The kinase activity of ULK-1 is required for autophagy induction though phosphorylating Beclin-1 (Ser15) to enhance a pro-autophagy VPS34-ATG14-Beclin-1 complex formation [64]. ULK-1 can be phosphorylated at Ser317 and Ser777 to induce autophagy via 5′-AMP-activated protein kinase (AMPK), while autophagy can be inhibited by ULK-1 phosphorylation at Ser757 via mammalian target of rapamycin (mTOR) [40]. Accordingly, we investigated the expression levels of inhibitory ULK-1 (Ser757) and Beclin-1 (Ser15) as downstream effectors of AKT. The activated AKT (p-AKT) inhibited autophagy in DN mice by increasing ULK-1 phosphorylation (Ser757) and decreasing Beclin-1 phosphorylation (Ser15), whereas P2Y2R deficiency attenuated AKT activation and restored autophagy activity.

In addition, recent studies on diabetes have reported that downregulation of SIRT-1 aggravates the pathogenesis of DN by inhibiting FOXO3a-mediated transcription of autophagy-regulatory genes [1,8,11]. Considering that SIRT-1 and FOXO3a signalling play key roles in autophagy induction [1,38,40], we examined the effect of P2Y2R deficiency on the SIRT-1 and FOXO3a pathways in DN. We found that both SIRT-1 and FOXO3a expression was significantly downregulated in DN, but KO mice restored the expression and promoted FOXO3a-mediated transcription of autophagy-regulatory genes. Taken together, P2Y2R contributes to AKT and SIRT-1/FOXO3a-mediated autophagy dysfunction, leading to the development of DN.

There are several limitations in the current study. The autophagy deficiency was evaluated only by protein and gene expression levels in global P2Y2R KO mice. We did not manipulate autophagy signalling using either silencing of key regulatory factors or stimulating of autophagy activity to confirm the processes mediated by P2Y2R. Moreover, further studies are required to validate the renal cell type-specific function of P2Y2R using conditional KO or region-specific induction for a precise therapeutic application in patients with DN.

In summary, P2Y2R promotes glomerulopathy, interstitial fibrosis, renal tubular injury and apoptosis through downregulating autophagy activity in DN via AKT/FOXO3a and SIRT-1 signalling pathways. Conversely, P2Y2R deficiency reverses these changes by activating autophagy response, thus improving the renal function. The upregulation of AKT phosphorylation plays a central role in the pathogenesis of DN by triggering renal apoptosis and negatively regulating FOXO3a transcriptional activity necessary for autophagy induction. Collectively, our study suggests that P2Y2R acts as a potential pathogenic mediator of DN, and blocking P2Y2R ameliorates the development of DN by altering AKT/FOXO3a and SIRT-1 signalling. Thus, manipulating P2Y2R may help to identify a novel therapeutic strategy for treating DN.

AUTHOR CONTRIBUTIONS

Conceptualisation: HK, SWP; data curation: TD, SRK, HK; formal analysis: TD, HK; funding acquisition: SWP; investigation: TD, SRK, EJP, JJ, KJ; methodology: TD, HK, SPY, HJK; project administration: HK, SWP; supervision: SWP; roles/writing - original draft: TD; writing - review and editing: HK, SWP.

CONFLICT OF INTEREST

The authors declare no conflicts of interest.

APPENDIX A. SUPPLEMENTARY DATA

Supplementary data to this article can be found online at https://doi.org/10.1016/j.molmet.2020.101089.

REFERENCES

[1] Ding, Y., Choi, M.E., 2015. Autophagy in diabetic nephropathy. Journal of Endocrinology 224(1):R15—R30.

[2] Jefferson, J.A., Shankland, S.J., Pichler, R.H., 2008. Proteinuria in diabetic kidney disease: a mechanistic viewpoint. Kidney International 74(1):22—36.

[3] Su, J., Li, S.J., Chen, Z.H., Zeng, C.H., Zhou, H., Li, L.S., et al., 2010. Evaluation of podocyte lesion in patients with diabetic nephropathy: Wilms' tumor-1 protein used as a podocyte marker. Diabetes Research and Clinical Practice 87(2):167—175.

[4] Collins, A.J., Foley, R.N., Chavers, B., Gilbertson, D., Herzog, C., Ishani, A., et al., 2014. US renal data system 2013 annual data report. American Journal of Kidney Diseases 63(1 Suppl):A7.

[5] Klionsky, D.J., Emr, S.D., 2000. Autophagy as a regulated pathway of cellular degradation. Science 290(5497):1717—1721.

[6] Kume, S., Koya, D., Uzu, T., Maegawa, H., 2014. Role of nutrient-sensing signals in the pathogenesis of diabetic nephropathy. BioMed Research International 2014:315494.

[7] Kume, S., Koya, D., 2015. Autophagy: a novel therapeutic target for diabetic nephropathy. Diabetes & Metabolism J 39(6):451—460.

[8] Tanaka, Y., Kume, S., Kitada, M., Kanasaki, K., Uzu, T., Maegawa, H., et al., 2012. Autophagy as a therapeutic target in diabetic nephropathy. Experimental Diabetes Research 2012:628978.

[9] Murtaza, G., Khan, A.K., Rashid, R., Muneer, S., Hasan, S.M.F., Chen, J., 2017. FOXO transcriptional factors and long-term living. Oxidative Medicine and Cellular Longevity 2017:3494289.

[10] Daitoku, H., Sakamaki, J., Fukamizu, A., 2011. Regulation of FoxO transcription factors by acetylation and protein-protein interactions. Biochimica et Biophysica Acta 1813(11):1954—1960.

[11] Wang, W., Sun, W., Cheng, Y., Xu, Z., Cai, L., 2019. Role of sirtuin-1 in diabetic nephropathy. Journal of Molecular Medicine (Berlin) 97(3):291—309.

[12] Menzies, R.I., Tam, F.W., Unwin, R.J., Bailey, M.A., 2017. Purinergic signaling in kidney disease. Kidney International 91(2):315—323.

[13] Arulkumaran, N., Turner, C.M., Sixma, M.L., Singer, M., Unwin, R., Tam, F.W., 2013. Purinergic signaling in inflammatory renal disease. Frontiers in Physiology 4:194.

Original Article

[14] Solini, A., Usuelli, V., Fiorina, P., 2015. The dark side of extracellular ATP in kidney diseases. Journal of the American Society of Nephrology 26(5):1007—1016.

[15] Vallon, V., Rieg, T., 2011. Regulation of renal NaCl and water transport by the ATP/UTP/P2Y2 receptor system. American Journal of Physiology - Renal Physiology 301(3):F463—F475.

[16] Zhang, Y., Pop, I.L., Carlson, N.G., Kishore, B.K., 2012. Genetic deletion of the P2Y2 receptor offers significant resistance to development of lithium-induced polyuria accompanied by alterations in PGE2 signaling. American Journal of Physiology - Renal Physiology 302(1):F70—F77.

[17] Harada, H., Chan, C.M., Loesch, A., Unwin, R., Burnstock, G., 2000. Induction of proliferation and apoptotic cell death via P2Y and P2X receptors, respectively, in rat glomerular mesangial cells. Kidney International 57(3):949—958.

[18] Kraus, A., Grampp, S., Goppelt-Struebe, M., Schreiber, R., Kunzelmann, K., Peters, D.J., et al., 2016. P2Y2R is a direct target of HIF-1alpha and mediates secretion-dependent cyst growth of renal cyst-forming epithelial cells. Purinergic Signalling 12(4):687—695.

[19] Schwiebert, E.M., Wallace, D.P., Braunstein, G.M., King, S.R., Peti-Peterdi, J., Hanaoka, K., et al., 2002. Autocrine extracellular purinergic signaling in epithelial cells derived from polycystic kidneys. American Journal of Physiology - Renal Physiology 282(4):F763—F775.

[20] Solini, A., Iacobini, C., Ricci, C., Chiozzi, P., Amadio, L., Pricci, F., et al., 2005. Purinergic modulation of mesangial extracellular matrix production: role in diabetic and other glomerular diseases. Kidney International 67(3):875—885.

[21] Hohenstein, B., Renk, S., Lang, K., Daniel, C., Freund, M., Leon, C., et al., 2007. P2Y1 gene deficiency protects from renal disease progression and capillary rarefaction during passive crescentic glomerulonephritis. Journal of the American Society of Nephrology 18(2):494—505.

[22] Bar, I., Guns, P.J., Metallo, J., Cammarata, D., Wilkin, F., Boeynams, J.M., et al., 2008. Knockout mice reveal a role for P2Y6 receptor in macrophages, endothelial cells, and vascular smooth muscle cells. Molecular Pharmacology 74(3):777—784.

[23] Burnstock, G., Evans, L.C., Bailey, M.A., 2014. Purinergic signalling in the kidney in health and disease. Purinergic Signalling 10(1):71—101.

[24] Rennert, L., Zschiedrich, S., Sandner, L., Hartleben, B., Cicko, S., Ayata, C.K., et al., 2018. P2Y2R signaling is involved in the onset of glomerulonephritis. Frontiers in Immunology 9:1589.

[25] Kim, H., Dusabimana, T., Kim, S.R., Je, J., Jeong, K., Kang, M.C., et al., 2018. Supplementation of abelmoschus manihot ameliorates diabetic nephropathy and hepatic steatosis by activating autophagy in mice. Nutrients 10(11).

[26] Ling, L., Yang, M., Ding, W., Gu, Y., 2019. Ghrelin attenuates UUO-induced renal fibrosis via attenuation of Nlrp3 inflammasome and endoplasmic reticulum stress. American Journal of Translational Research 11(1):131—141.

[27] Souza, A.C., Tsuji, T., Baranova, I.N., Bocharov, A.V., Wilkins, K.J., Street, J.M., et al., 2015. TLR4 mutant mice are protected from renal fibrosis and chronic kidney disease progression. Physics Reports 3(9).

[28] Zhong, F., Chen, Z., Zhang, L., Xie, Y., Nair, V., Ju, W., et al., 2018. Tyro3 is a podocyte protective factor in glomerular disease. JCI Insight 3(22).

[29] Yang, J., Zhu, F., Wang, X., Yao, W., Wang, M., Pei, G., et al., 2016. Continuous AMD3100 treatment Worsens renal fibrosis through regulation of bone marrow derived pro-angiogenic cells homing and T-cell-related inflammation. PloS One 11(2):e0149926.

[30] Zhang, Y., Li, Q., Liu, D., Huang, Q., Cai, G., Cui, S., et al., 2016. GDF11 improves tubular regeneration after acute kidney injury in elderly mice. Scientific Reports 6:34624.

[31] Takagaki, Y., Shi, S., Katoh, M., Kitada, M., Kanasaki, K., Koya, D., 2019. Dipeptidyl peptidase-4 plays a pathogenic role in BSA-induced kidney injury in diabetic mice. Scientific Reports 9(1):7519.

[32] Lavoz, C., Matus, Y.S., Orejudo, M., Carpio, J.D., Droguett, A., Egido, J., et al., 2019. Interleukin-17A blockade reduces albuminuria and kidney injury in an accelerated model of diabetic nephropathy. Kidney International 95(6):1418—1432.

[33] Castillo-Rodriguez, E., Fernandez-Prado, R., Martin-Cleary, C., Pizarro-Sanchez, M.S., Sanchez-Nino, M.D., Sanz, A.B., et al., 2017. Kidney injury marker 1 and neutrophil gelatinase-associated lipocalin in chronic kidney disease. Nephron 136(4):263—267.

[34] Sabbisetti, V.S., Waikar, S.S., Antoine, D.J., Smiles, A., Wang, C., Ravisankar, A., et al., 2014. Blood kidney injury molecule-1 is a biomarker of acute and chronic kidney injury and predicts progression to ESRD in type I diabetes. Journal of the American Society of Nephrology 25(10):2177—2186.

[35] Burlaka, I., Nilsson, L.M., Scott, L., Holtback, U., Eklof, A.C., Fogo, A.B., et al., 2016. Prevention of apoptosis averts glomerular tubular disconnection and podocyte loss in proteinuric kidney disease. Kidney International 90(1):135—148.

[36] Verzola, D., Gandolfo, M.T., Ferrario, F., Rastaldi, M.P., Villaggio, B., Gianiorio, F., et al., 2007. Apoptosis in the kidneys of patients with type II diabetic nephropathy. Kidney International 72(10):1262—1272.

[37] Wang, X., Meng, L., Zhao, L., Wang, Z., Liu, H., Liu, G., et al., 2017. Resveratrol ameliorates hyperglycemia-induced renal tubular oxidative stress damage via modulating the SIRT1/FOXO3a pathway. Diabetes Research and Clinical Practice 126:172—181.

[38] Dusabimana, T., Kim, S.R., Kim, H.J., Park, S.W., Kim, H., 2019. Nobiletin ameliorates hepatic ischemia and reperfusion injury through the activation of SIRT-1/FOXO3a-mediated autophagy and mitochondrial biogenesis. Experimental & Molecular Medicine 51(4):1—16.

[39] Nho, R.S., Hergert, P., 2014. FoxO3a and disease progression. World Journal of Biological Chemistry 5(3):346—354.

[40] Yao, F., Zhang, M., Chen, L., 2016. 5'-Monophosphate-activated protein kinase (AMPK) improves autophagic activity in diabetes and diabetic complications. Acta Pharmaceutica Sinica B 6(1):20—25.

[41] Fotino, C., Vergani, A., Fiorina, P., Pileggi, A., 2015. P2X receptors and diabetes. Current Medicinal Chemistry 22(7):891—901.

[42] Chen, K., Zhang, J., Zhang, W., Zhang, J., Yang, J., Li, K., et al., 2013. ATP-P2X4 signaling mediates NLRP3 inflammasome activation: a novel pathway of diabetic nephropathy. The International Journal of Biochemistry & Cell Biology 45(5):932—943.

[43] Solini, A., Menini, S., Rossi, C., Ricci, C., Santini, E., Blasetti Fantauzzi, C., et al., 2013. The purinergic 2X7 receptor participates in renal inflammation and injury induced by high-fat diet: possible role of NLRP3 inflammasome activation. The Journal of Pathology 231(3):342—353.

[44] Taylor, S.R., Turner, C.M., Elliott, J.I., McDaid, J., Hewitt, R., Smith, J., et al., 2009. P2X7 deficiency attenuates renal injury in experimental glomerulonephritis. Journal of the American Society of Nephrology 20(6):1275—1281.

[45] Turner, C.M., Tam, F.W., Lai, P.C., Tarzi, R.M., Burnstock, G., Pusey, C.D., et al., 2007. Increased expression of the pro-apoptotic ATP-sensitive P2X7 receptor in experimental and human glomerulonephritis. Nephrology Dialysis Transplantation 22(2):386—395.

[46] Turner, C.M., King, B.F., Srai, K.S., Unwin, R.J., 2007. Antagonism of endogenous putative P2Y receptors reduces the growth of MDCK-derived cysts cultured in vitro. American Journal of Physiology - Renal Physiology 292(1):F15—F25.

[47] Turner, C.M., Ramesh, B., Srai, S.K., Burnstock, G., Unwin, R.J., 2004. Altered ATP-sensitive P2 receptor subtype expression in the Han:SPRD cy/+ rat, a model of autosomal dominant polycystic kidney disease. Cells Tissues Organs 178(3):168—179.

[48] Ji, X., Naito, Y., Hirokawa, G., Weng, H., Hiura, Y., Takahashi, R., et al., 2012. P2X(7) receptor antagonism attenuates the hypertension and renal injury in Dahl salt-sensitive rats. Hypertension Research 35(2):173—179.

[49] Osmond, D.A., Inscho, E.W., 2010. P2X(1) receptor blockade inhibits whole kidney autoregulation of renal blood flow in vivo. American Journal of Physiology - Renal Physiology 298(6):F1360—F1368.

[50] Liu, N., Tolbert, E., Pang, M., Ponnusamy, M., Yan, H., Zhuang, S., 2011. Suramin inhibits renal fibrosis in chronic kidney disease. Journal of the American Society of Nephrology 22(6):1064—1075.

[51] Friedman, D.J., Rennke, H.G., Csizmadia, E., Enjyoji, K., Robson, S.C., 2007. The vascular ectonucleotidase ENTPD1 is a novel renoprotective factor in diabetic nephropathy. Diabetes 56(9):2371—2379.

[52] Grgic, I., Campanholle, G., Bijol, V., Wang, C., Sabbisetti, V.S., Ichimura, T., et al., 2012. Targeted proximal tubule injury triggers interstitial fibrosis and glomerulosclerosis. Kidney International 82(2):172—183.

[53] He, X., Zhang, T., Tolosa, M., Goru, S.K., Chen, X., Misra, P.S., et al., 2019. A new, easily generated mouse model of diabetic kidney fibrosis. Scientific Reports 9(1):12549.

[54] Ma, J., Chadban, S.J., Zhao, C.Y., Chen, X., Kwan, T., Panchapakesan, U., et al., 2014. TLR4 activation promotes podocyte injury and interstitial fibrosis in diabetic nephropathy. PloS One 9(5):e97985.

[55] Xiao, L., Zhu, X., Yang, S., Liu, F., Zhou, Z., Zhan, M., et al., 2014. Rap1 ameliorates renal tubular injury in diabetic nephropathy. Diabetes 63(4):1366—1380.

[56] Wang, Z., Choi, M.E., 2014. Autophagy in kidney health and disease. Antioxidants and Redox Signaling 20(3):519—537.

[57] Tagawa, A., Yasuda, M., Kume, S., Yamahara, K., Nakazawa, J., Chin-Kanasaki, M., et al., 2016. Impaired podocyte autophagy exacerbates proteinuria in diabetic nephropathy. Diabetes 65(3):755—767.

[58] Huang, S.S., Ding, D.F., Chen, S., Dong, C.L., Ye, X.L., Yuan, Y.G., et al., 2017. Resveratrol protects podocytes against apoptosis via stimulation of autophagy in a mouse model of diabetic nephropathy. Scientific Reports 7:45692.

[59] Xu, J., Liu, L.Q., Xu, L.L., Xing, Y., Ye, S., 2020. Metformin alleviates renal injury in diabetic rats by inducing Sirt1/FoxO1 autophagic signal axis. Clinical and Experimental Pharmacology and Physiology 47(4):599—608.

[60] Huang, X., Liu, G., Guo, J., Su, Z., 2018. The PI3K/AKT pathway in obesity and type 2 diabetes. International Journal of Biological Sciences 14(11):1483—1496.

[61] Silva, G.B., Garvin, J.L., 2009. Akt1 mediates purinergic-dependent NOS3 activation in thick ascending limbs. American Journal of Physiology - Renal Physiology 297(3):F646—F652.

[62] Xue, M., Cheng, Y., Han, F., Chang, Y., Yang, Y., Li, X., et al., 2018. Triptolide attenuates renal tubular epithelial-mesenchymal transition via the MiR-188-5p-mediated PI3K/AKT pathway in diabetic kidney disease. International Journal of Biological Sciences 14(11):1545—1557.

[63] Nam, S.,A., Kim, W.Y., Kim, J.W., Park, S.H., Kim, H.L., Lee, M.S., et al., 2019. Autophagy attenuates tubulointerstital fibrosis through regulating transforming growth factor-beta and NLRP3 inflammasome signaling pathway. Cell Death & Disease 10(2):78.

[64] Russell, R.C., Tian, Y., Yuan, H., Park, H.W., Chang, Y.Y., Kim, J., et al., 2013. ULK1 induces autophagy by phosphorylating Beclin-1 and activating VPS34 lipid kinase. Nature Cell Biology 15(7):741—750.